Journal of Theoretical and Applied Information Technology
15th July 2019. Vol.97. No 13

ISSN: 1992-8645 www.jatit.org E-ISSN: 1817-3195

INTEGRATION OF SPECTRAL MIXTURE ANALYSIS FROM THAICHOTE SATELLITE DATA TO IDENTIFY GREEN VEGETATION CANOPY DENSITY

[1] SUNSANEE MANEECHOT, [1,2] RASAMEE SUWANWERAKAMTORN
[1] Department of Computer Science, Faculty of Science, Khon Kaen University, Khon Kaen Thailand
[2] Geo-informatics Centre for Development of Northeast Thailand, Faculty of Science,
Khon Kaen University, Khon Kaen, Thailand
E-mail: [1]sunsanee.maneechot@gmail.com, [2]rasamee@kku.ac.th

ABSTRACT

Many studies have assessed forest canopy density which is a major factor in evaluating forest status and is an important indicator of possible management interventions. Using satellite remote sensing has proved cost effective means of mapping and monitoring environment in terms of vegetation and other ecological issues. In this study, we demonstrated a new method based on the spatial integration which was operated by combining a spectral mixture analysis (SMA) into multispectral bands to create the green vegetation canopy density (GVCD). The GVCD approach was used to classify the forest canopy density in the Phu Phan National Park, Sakon Nakhon province where it is located in the Northeast of Thailand; it covers an area of approximately 66,470 hectares. THAICHOTE multispectral image with 15-m resolution acquired in 2015 was used in the analyzing process. A spatial integration of green vegetation fraction (GV) and soil fraction derived from SMA technique and scaled shadow index (SSI) was digitally performed and analyzed to classify GVCD. In addition, ground truth investigation of 48 exemplars was conducted to establish the reliability of model used for GVCD. The agreement between the results and the ground observation was reliably obtained with Kappa coefficient of 0.68 and overall accuracy of 79.17%. The results showed the ability of GVCD approach measured by using the analyzed results of VD and SSI to calculate and detect the forest canopy density. This study also revealed the potentiality of THAICHOTE data in monitoring and identifying vegetation conditions.

Keywords: *Spectral Mixture Analysis (SMA); Green Vegetation Canopy Density (GVCD); Green Vegetation fraction (GV); Soil fraction; THAICHOTE data*

1. INTRODUCTION

Forest canopy density (FCD) is one of the most important parameters for evaluating forest cover status. It is an important parameter for possible planning, implementation of rehabilitation and overall management programs of forest cover [1]. Remote sensing has been widely used with varying degrees of success to quantify characteristics of spatial forest structure such as crown cover, tree density, tree diameter, basal area, biomass, and leaf area index. Green vegetation canopy density (GVCD) is also one of the tools to identify the forest canopy density with the integration of spectral mixture analysis (SMA). The study area was at the Phu Phan National Park where it is located in the north of Phu Phan Mountains in the north-eastern region of Thailand. Since in the past until now, this conservative forest has been continuously disturbed because its boundary connects to villages of which their transportation conditions have been well-developed, so it has also provided the convenience in inter-villages transportation and in the access to the National Park. Moreover, the villages around the National Park have been highly expanded, so this affects the demands of land and forest uses in a larger number. The majority of the forests in this National Park characterize into deciduous forests; they are dry dipterocarp forest and mixed deciduous forest. In this case, they become great fuels, and they cause wildfire spreading all over area of the National Park. In some areas, there are wildfire occurred every year until they eventually become degraded forests.

The FCD is based on the data derived from an integration of Vegetation Index (VI), Bare Soil Index (BI), Shadow Index (SI), and Thermal Index (TI), and it has been successfully applied in a number of countries in tropical regions [2]. The mentioned

ISSN: 1992-8645 www.jatit.org E-ISSN: 1817-3195

indices are normalized into the same range; and the canopy density has been computed in percentage for each pixel by using three techniques for FCD mapping with satellite data: visual interpretation (VI), object oriented image segmentation (OOIS) and FCD model [3]. In comparing the above techniques, the FCD model has been found to be the better density mapping technique than other two in terms of accuracy, efficiency and high correlation with ground estimation. The study was conducted in a comparison of three classification approaches to estimate FCD of tropical mixed deciduous vegetation [4]. The three classification approaches composed of maximum likelihood classification (MLC), multiple linear regressions (MLR) and FCD Mapper. The study attempted to monitor the forest deforestation or degradation in a natural forest by using FCD Model. This model involved bio-spectral phenomenon modeling and analysis utilizing data derived from the following three indices: vegetation, bare soil and shadow. The results proved to be effective means for measuring forest cover assessment and less information of ground validation [5]. An integrated remote sensing and geographic information system tools showed the density of forest cover. A combined FCD and Digital Elevation Model (DEM) of TERRA satellite ASTER (Advanced Space borne Thermal Emission and Reflection Radiometer) was adopted to study the variation of dense forest in a large scale. The FCD was calculated based on bare soil index, shadow index and vegetation index, yielding the overall accuracy of 86 to 90% [6]. The analysis method by weighted overlay was applied to survey the forest canopy density. Various indices such as normalized difference vegetation index (NDVI), bareness index, shadow index and perpendicular vegetation index (PVI) etc. were used. A greater weight was assigned for higher concentration of vegetation whereas a lesser weight was assigned for lower concentration of vegetation. [7].

A spectral vegetation index (VI) is usually a single number derived from the spectral reflectance of two or more bands. Because a VI is proportional to the value of biophysical parameters such as the leaf area index (LAI), green vegetation fraction (GV), net primary productivity (NPP), and fraction of absorbed photosynthetically active radiation (APAR), it is commonly used to indicate vegetation vigor and amount. A large number of spectral VIs have been developed and used in remote sensing. Well-known VIs including normalized difference vegetation index (NDVI) [8], soil adjusted vegetation index (SAVI) [9], global environmental monitoring index (GEMI) [10], modified SAVI (MSAVI2) [11], and enhanced vegetation index (EVI) [12] have potential for extensive application. Each spectral VI has its own merits and limitations. For example, NDVI equation is a non-linear transformation of the simple ratio between near-infrared and red band; it is the major cause for saturation in high biomass situations. Moreover, NDVI is very sensitive to canopy background variations with NDVI degradation particularly strong with higher canopy background brightness [9].

VI is a traditional pixel-based classification method that assigns a pixel to a single class. Because of the real conditions, the surface of the land cover which consists of many objects is mixed together. When the sensor system detects surface conditions, it is found that in one pixel, the object is represented by more than one object. Therefore, this affects the efficiency in using remote sensing data for land use and land cover classification [13]. Spectral Mixture Analysis (SMA) is a sub-pixel classification technique based on the spectral responses of land cover components. It is used to detect spectral responses of materials that are smaller than an image pixel. It is also useful for detecting materials that cover larger areas but are mixed with other materials that complicate accurate classification. SMA assumes that each image spectrum is a linear combination of a few pure spectra, so-called endmembers [14]. SMA models of vegetation consist of four endmembers: green vegetation (GV), non-photosynthetic vegetation (NPV), soil, and shade fractions within each pixel. The analysis result is an estimate of the percentage cover of each endmember for every pixel. The GV fraction is correlated with NDVI, but has been demonstrated to be a slightly better predictor of photosynthetic vegetation quantity in semi-arid systems [15]. SMA, as a tool for vegetation cover analysis receives much attention in the last decades. Since SMA can be used to provide a full spectrum measurement of vegetation response, SMA fractions are more robust than traditional vegetation indices [15]–[17]. The study attempted to apply linear spectral mixture model (LSMM) approach to classify successional and mature forests by using Landsat Thematic Mapper (TM) imagery in Amazon. This indicated that LSMM approach provided a better separating ability between successional and mature forests [18]. The study also examined the value of SMA using Landsat (TM) data for improving LULC classification accuracy in a moist tropical area in Rondbnia, Brazil. A maximum likelihood classifier was also used to classify fraction images into seven LULC classes. The results of this study indicated

ISSN: 1992-8645 www.jatit.org E-ISSN: 1817-3195

that reducing correlation between image bands and using four endmembers has improved classification accuracy [19]. Another study employed spectral unmixing for forest mapping approach by using multi-temporal Landsat imagery to quantify the percentage of basal area for ten common tree species/genera across northern New York and Vermont. These results showed that a combination of multi-temporal imagery, spectral unmixing, and rule-based classification techniques provided more detailed and accurate forest mapping [20]. Furthermore, the study attempted to monitor the deforestation or degradation in a natural forest by using SMA. The study demonstrated a method to classify forest cover changes associated with deforestation and degradation across the entire region for the years 2000-2010 using Landsat satellite imagery in the Brazilian Amazon. In combining SMA, normalized difference fraction index, and knowledge-based decision tree classification, they mapped and assessed the accuracy to quantify forest (0.97), deforestation (0.85) and forest degradation (0.82) with an overall accuracy of 0.92. [21] The study used three techniques – object-based oriented classification (OBIA), SMA and change vector analysis (CVA) – to study the desertification processes, and driving variables influencing land degradation and vegetation cover within White Nile State, Sudan during different years. The paper provided that SMA technique was powerful for characterization and mapping of land degradation in the study area by offering more detailed information at sub-pixel level [22]. Other studies applied SMA in combination with GIS techniques such as [23] propose a new method for monitoring areas affected by selective logging in one of the hotspots of Mato Grosso state in the Brazilian Amazon based on a combination of object-based and pixel-based classification approaches applied on remote sensing data. The use of fraction images derived from Landsat imagery was also an essential step to identify logging openings as it allows highlighting features at a sub-pixel level. The result indicated that their method provided a feasible means of assessing forest disturbances consistently and allowed assessing deforestation and forest disturbances due to selective logging.

Based on previous work in forest canopy density, spectral mixture analysis and existing forest mapping strategies, the objective of this study was to demonstrate a new method based on the spatial integration operated by combining a spectral mixture analysis (SMA) into multispectral bands to create the green vegetation canopy density (GVCD) in order to classify the forest canopy density. Moreover, this study also conducted a statistical analysis to show a relationship between green vegetation fraction (GV) and soil fraction derived from SMA techniques, and different vegetation indices.

2. STUDY AREA

The Phu Phan National Park is located in the north of Phu Phan Mountains in the north-eastern region of Thailand. It is located between latitude 16º 44' N to 17º16 ' N and longitude 103º45 ' E to104 º 03' E; the area is approximately 66,470 hectares in total. The terrain of national park consists of a range of high mountains from the north to the south. The geological structure characterizes into sandstones, 200 – 567 meters above sea level. The characteristics of topography inside the park are categorized into 2 regions. The mountains in the north region feature into an inverted shape pan. General areas are average slopes at about 15 percent and there are some small mountains which characterize in high slopes in some patches. On the other hand, the mountains in the south region are average slopes at about 30 percent and they are one of the important water sources.

The climate is sub-tropical with three seasons: rainy, winter, and summer. Rainy season starts from June to October. There is the highest average rainfall in August; 367.7 millimeters of average rainfall and 94% of average relative humidity. Winter season starts from November to February. The general weather in this season is pretty cool. There is a very little average rainfall, not over 20 millimeters per month. The lowest average temperature is at 22.6 °C. Hot season starts from March to May. The average temperature is at 30.1 °C. The Phu Phan National Park has deciduous forests covering the major area of the park, 41.58 percent of the overall area. This forest type is mostly found in the central of the park up to the north at the 200-400 meters above sea level. The most secondly found forest type is the mixed deciduous forest, 22.16 percent of the overall area. It is mostly found in the south of the park. The area consists of plains and plateaus. Another type of forest found in this park is the dry evergreen forest, 17.49 percent of the overall area. It is a large forest which covers the central area and a bit down to the south of the park at the above sea level of more than 400 meters high.

3. MATERIALS AND METHODS

In this study, we used multispectral THAICHOTE data. It had been obtained from the Geo-Informatics and Space Technology

ISSN: 1992-8645 www.jatit.org E-ISSN: 1817-3195

Development Agency (Public Organization) (GISTDA) acquired on the dry season. For image pre-processing, the data was transformed to top-of-atmosphere (TOA) radiance, and the geometric correction was performed. The analysis composed of 5 steps. The first step generated forest mask which aimed at excluding non-forest areas by using the maximum likelihood classification. The second step calculated vegetation indices including EVI, NDVI, SAVI, GEMI, and MSAVI2. The third step generated endmembers by using the spectral unmixing method. There were four endmembers including soil, shade, Green Vegetation (GV), and Non-photosynthetic vegetation (NPV). After that, we randomly sampled points for all indices to assess the relationship based on Pearson's correlation. The forth step integrated 2 fractions (GV fraction and Soil fraction) from SMA technique and Scale Shadow Index (SSI) to generate the Green Vegetation Canopy Density (GVCD). Finally, ground truth was employed for validating GVCD approach. Figure 2 shows the flowchart of the study.

3.1 Dataset

In this study, THAICHOTE satellite data obtained on March 6, 2015 and containing the 15 meters spatial resolution in multispectral band including Blue (0.45-0.52 µm.) Green (0.53-0.60 µm.) Red (0.62-0.69 µm.) and Near-infrared (0.77-0.90 µm.) was used.

3.2 Image pre-processing

3.2.1 The atmospheric correction

The atmospheric correction consisted of two steps. First, the atmospheric correction converted the digital numbers (DN) into a spectral radiance at a sensor's aperture (L_λ) by using the sensor's gains. The gains of THAICHOTE were given on their image header files, and the at-sensor spectral radiances of THAICHOTE for each band were calculated by using the following equation.

$$L^i_{\lambda Thaichote} = \frac{DN_i}{Gain_i} \quad (1)$$

Where $L^i_{\lambda Thaichote}$ is the at-sensor spectral radiance of THAICHOTE for band i ($Wm^{-2}\ sr^{-1}\ \mu m^{-1}$)

DN_i is the digital number of band i;

$Gain_i$ is the THAICHOTE gain for band i

The second step involved the conversion of spectral radiance at the sensor's aperture (L_λ) into the exo-atmospheric top-of-the-atmosphere (TOA) reflectance (ρTOA); it was computed based on the following equation [24]. The data from THAICHOTE is shown in Table 1.

$$\rho = \frac{\pi * L^i_\lambda * d^2}{ESUN^i_\lambda * cos\theta_{SAT}} \quad (2)$$

Where ρ is planetary directional TOA reflectance for lambertian surfaces [unitless]

L^i_λ is THAICHOTE at-sensor spectral radiance for band i ; [$Wm^{-2}\ sr^{-1}\ \mu m^{-1}$]

$ESUN^i_\lambda$ is THAICHOTE Mean exo-atmospheric solar irradiance for band i [$Wm^{-2}\ sr^{-1}\ \mu m^{-1}$]

d is an Earth-Sun distance [astronomical units]

θ_{SAT} is solar zenith angle or the value of the sine function of the solar elevation angle.

Table 1: THAICHOTE spectral ranges and mean exo-atmospheric solar irradiances ($ESUN^i_\lambda$)

Spectral Range (nm)	Band	$ESUN^i_\lambda$ [$Wm^{-2}\ sr^{-1}\ \mu m^{-1}$]
450-520	Blue	1983
530-600	Green	1813
620-690	Red	1552
770-900	Near-infared	962

3.2.2 Geometric correction

Information in this study was derived from the 2002 aerial orthophotography (scale 1:4000) and THAICHOTE multispectral scene (15m. resolution) acquired on March 6, 2015. Image to image registration had been performed between the datasets, which were co-registered in UTM (WGS-84) coordinate system by using nearest-neighborhood algorithm, with an RSME error of less than 0.5 pixels.

3.3 Building forest masks

Before the next stage of the study analysis was operated, building forest masks from THAICHOTE image by using the maximum likelihood classification approach was initially conducted for classifying the area types of the forests (dense forest, medium forest and open forest) and the area types of non-forests (agricultural areas and water body) including clouds and shadows. However, the area types of non-forests were not analyzed.

ISSN: 1992-8645 www.jatit.org E-ISSN: 1817-3195

3.4 Vegetation Indices

Vegetation Indices were used to calculate the difference between the two bands or more. The calculation was used to classify whether in which areas were covered by vegetation, and the bands correlated to the vegetation were RED band and Near-Infrared band.

Enhanced Vegetation Index (EVI) was one of the fundamental products for MODIS Satellite which was developed to adjust the image enhancement and to monitor vegetation by classifying forest canopy. It was a modified NDVI with a soil adjustment factor L and two coefficients *C1* and *C2*, which described the use of the blue band in the correction of the red band for atmospheric aerosol scattering. This VI had improved sensitivity to high biomass regions and reduced atmospheric influence. [12]

$$EVI = G\,\frac{NIR - RED}{NIR + C_1R - C_2B + L}\,(1 + L) \tag{3}$$

Where $C_1 = 6$, $C_2 = 7.5$, $L = 0.5$

Normalized Difference Vegetation Index (NDVI) was proposed by [8]. It was applied to search and investigate about vegetation by classifying types of vegetation. It was calculated from the ratio of difference between near infrared and red bands normalized by the sum of those bands. The measurement scale has the desirable property of ranging from -1 to 1. The scale of NDVI close to -1 means that area was covered by vegetation less than soil while the scale of NDVI close to +1 means that area was dense vegetation canopy or forest.

$$NDVI = \frac{NIR - RED}{NIR + RED} \tag{4}$$

Soil-Adjusted Vegetation Index (SAVI) was proposed by [9]. It was intended to minimize the effects of soil background on the vegetation signal by incorporating a constant soil adjustment factor L into the denominator of the NDVI equation. L varied with the reflectance characteristics of the soil (e.g., color and brightness). The L factor was chosen based on the density of the vegetation. In cases of very low vegetation, the use of an L factor of 1.0 was suggested, for intermediate at 0.5, and for high density at 0.25.

$$SAVI = \frac{(NIR - RED)}{(NIR + RED + L)} \times (1 + L) \tag{5}$$

SAVI was between 1 - to1 + . The area which was covered by vegetation less than soil showed the scale nearly at -1 while the area of dense vegetation canopy showed the scale nearly at +1.

Global Environmental Monitoring Index (GEMI) was developed by [10], and it was a distance-based approach and non-linear vegetation index developed to be less sensitive to atmospheric effects. Although GEMI was initially intended to minimize atmospheric effects, it was also a more sensitive index to soil background [11]. GEMI performed best when vegetation cover was sparse, where a decrease in the value of GEMI corresponded to an increase in crown cover [25].

$$GEMI = \frac{\eta(1 - 0.25\eta) - \rho RED - 0.125}{(1 - \rho RED} \tag{6}$$

$$\eta = \frac{2(\rho_{NIR}^2 - \rho_{RED}^2) + 1.5\rho NIR + 0.5\rho RED}{\rho NIR + \rho RED + 0.5} \tag{7}$$

Modified Soil-Adjusted Vegetation Indices (MSAVI-2) suggested by [11] were based on a modification of the *L* factor of the SAVI. It was intended to better correct the soil background brightness in different vegetation cover conditions. MSAVI-2, used an inductive *L* factor to: (i) remove the soil "noise" that was not cancelled out by the product of NDVI by WDVI, and (ii) correct values greater than 1. Thus, its use was limited for high vegetation density areas.

$$MSAVI2 = \frac{2pNIR + 1 - \sqrt{(2pNIR + 1)^2 - 8(pNIR - pRED)}}{2} \tag{8}$$

3.5 Spectral mixture analysis

SMA assumed that the image spectra were formed by a linear combination of N pure spectra, such that

$$R_i = \sum_{i=1}^{N} F_i R_{ib} + \varepsilon_b \tag{9}$$

Where R_i = reflectance of bandpass 'b', R_{ib} = reflectance value of endmember 'i' in bandpass 'b' (if an image is calibrated to reflectance, R_{ib} must be used instead), N=number of endmembers, F_i = fractional abundance of endmember 'i' and ε_b = error of the fit for bandpass 'b'

ISSN: 1992-8645 www.jatit.org E-ISSN: 1817-3195

A second equation may be used to constrain the sum of fractions to 1:

$$\sum_{i=1}^{N} F_i = 1 \quad (10)$$

Since spectral endmembers may be the result of mixing with different materials, fractional abundance of endmember 'i' may be less than 0 and greater than 1 although the overall fraction will be 1. It indicated that two materials may be combined, which would result in a negative or greater than 1 fraction. It did not necessarily mean that there were method errors [26].

The accuracy of the model was assessed either as an error in fraction residuals or as the root mean square error (RMSE) across the bands. To estimate the accuracy of the computed endmember fraction, an error image was computed by using the formula for the RMSE for an n-band image:

$$RMSE = \sqrt{\frac{1}{n} \cdot \sum_{i=1}^{n} (\varepsilon_i)^2} \quad (11)$$

The overall of the model was judged to be accurate if band residuals or RMS errors had low value and if the fraction was not lower than 0 or larger than 1.

Endmember selection was the most important step in SMA analysis because endmember was a spectral value representing the material in the earth's surface. In this study, the image-based selection of endmembers was used because they were easily obtained, and they represented spectra measured at the same scale as the image data [27]. The Pixel Purity Index (PPI) was presented as an alternative approach to select endmembers. This technique was based upon the principle that the spectral signature of a specific material was 'pure' (not compounded) [28]. Therefore, PPI was designed to identify the most spectrally extreme, different, or 'pure' pixels, which commonly corresponded to mixed endmembers [28], [29]. Spectral unmixing method was applied to determine the relative abundance of materials depicted in multispectral imagery based on the spectral characteristics of materials. The reflectance of each pixel in the image was assumed to be a linear combination of the reflectance of each material presented within the pixel. In this study, we generated the endmembers from THAICHOTE imagery in four bands (1 – 4). There were four endmembers including soil, shade, Green Vegetation (GV), and Non-photosynthetic vegetation (NPV).

In this analysis, we randomly sampled points representing multiple values for each vegetation index and GV, soil fraction of SMA techniques in the study site. We used those sampled index values to assess the relationship of all indices based on Pearson's correlation. The results of Pearson's correlation (Pearson's r) indicated that GV, soil fraction and vegetation indices were related.

3.6 Green vegetation canopy density model

GVCD approach is measured by using the analyzed results of VD and SSI to calculate for the forest canopy density with an integration of vegetation density (VD) and Scaled Shadow Index (SSI), based on the concept studied by [2]. In this study, some indices implemented differently from those of Rikimura model. Details of the adopted model are explained as the following steps.

3.6.1 Vegetation Density (VD)

Previous studies had applied NDVI and bare soil index (BI) to generate FCD model.

In this study, the results derived from two fractions of spectral mixture analysis, green vegetation fraction (GV) and soil fraction were employed to evaluate VI and BI respectively to detect VD.

Processing method was operated by using principal component analysis (PCA). The first principal component analysis (PCA1) between GV fraction (VI) and soil fraction (BI) was used because those two parameters carried high negative correlation. After that, the scales of zero percent point and a hundred percent point were set.

3.6.2 Scaled Shadow Index (SSI)

The Shadow Index (SI) was generated and used for identifying SSI [30] as shown in the following equation:

$$SI = ((256-B1) \times (256-B2) \times (256-B3))^{1/3} \quad (12)$$

Where B1 = Blue band, B2 = Green band, and B3 = Red band

The SSI can be produced by rescaling the SSI in the range between 0 and 100. 100% of SSI represents the highest possible shadow whereas the 0% one represents the opposite result.

Journal of Theoretical and Applied Information Technology
15th July 2019. Vol.97. No 13

ISSN: 1992-8645 www.jatit.org E-ISSN: 1817-3195

3.6.3 Green Vegetation Canopy Density (GVCD)

GVCD approach is measured by using the analyzed results of VD and SSI to calculate for the forest canopy density [2] as shown in the following equation:

$$GVCD = VD\ (SSI + 1)^{1/2} - 1 \quad (13)$$

The forest cover was interpreted into three classes based on GVCD: dense forest (>60%), medium forest (30-60%), and open forest (0-30%).

3.7 Validation

Forty eight plots of ground truth through field survey were employed for identifying GVCD. The distribution of the exemplars is depicted in Figure 3. The obtained result was used to establish a cross-tabulation in comparing the field-based classes and image-based classes for validation by which the kappa statistic was applied.

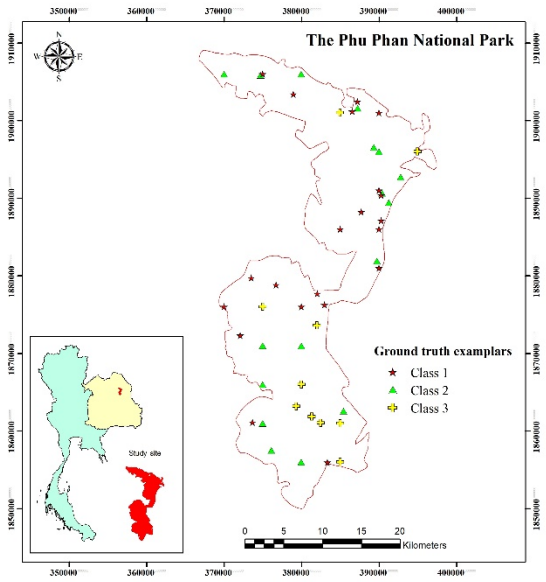

Figure 3: Ground Truth Exemplars

4. RESULT AND DISCUSSION

4.1 Endmember selection

The results from Spectral unmixing method consisted of image sets of four endmembers: GV, NPV, Soil and Shade images, and RMS error image. In this model, the RMSE was at 0.028. The SMA process showed land cover in percentages ranged from 1 to 100 percent.

Figure 4 representing GV fraction shows the lowest reflectance in red band and higher spectral reflectance in near-infrared band. Both NPV fraction and Soil fraction had reflectance increased continuously from blue band until near-infrared band, but NPV fraction had a lower reflectance. Shade fraction reflectance decreased continuously in blue band until red band and slightly increased in red band and near-infrared band.

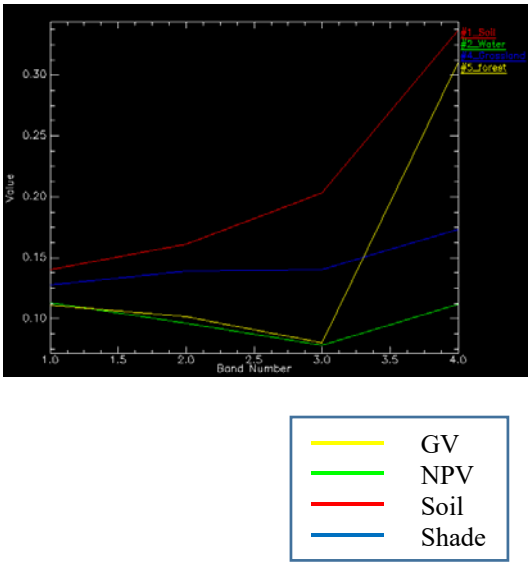

Figure 4: Reflectance characteristics of image endmembers: GV = green vegetation; NPV = non-photosynthetic vegetation.

4.2 Relationships among various vegetation indices

In this analysis, the relationships among EVI, SAVI, NDVI, MSAVI2, GEMI and GV, soil fraction derived from SMA technique in which they were retrieved from a THAICHOTE image acquired on March 6, 2015 were tested. Table 2 illustrates the relationships of various vegetation indices in the study site.

This correlation matrix (Table 2) demonstrates high correlation ($r \geq 0.92$) among all vegetation indices except for MSAVI2 which was a lowest correlation between all vegetation indices. The highest correlations were observed between EVI-SAVI, NDVI-EVI, NDVI-SAVI, and SAVI-GEMI ($r=0.99$). High correlation ($r \geq 0.96$) was also observed between GV-NDVI, GV-EVI, and GV-SAVI. The results were correspondent with the study of [31] in which the abilities of various vegetation indices were tested together with GV fraction. The study found that GV fraction had pretty high relationship with all vegetation indices ($r \geq 0.95$). On the other hand, the relationship between soil fraction and other vegetation indices was in high negative value ($r \geq 0.71$).

ISSN: 1992-8645 www.jatit.org E-ISSN: 1817-3195

4.3 Vegetation Density

The linear transformation performed the results in eigenvectors to generate the PC1 for THAICHOTE data with eigenvalues of 99.81%. The calculation is:

$$VD_{(PC1)} = - 0.90542 (GV) - 0.42451 (SOIL) \quad (14)$$

The obtained VD provided for input in creating the GVCD calculation.

4.4 Accuracy assessment of GVCD approach for forest classification

As for the validation of the result, a confusion matrix between ground truths of 48 locations and the classified GVCD based on the 2015 THAICHOTE imagery in Table 3 shows the agreement between the classes. The confusion matrix revealed that canopy classes were mapped with overall accuracy of 79.17% with 0.68 of kappa coefficient. The dense forest class was classified more accurately with a producer's accuracy of 100% than other canopy classes. Open forest and medium forest density classes showed fair accuracy levels at 76.19 % and 68.75%, respectively. The results gained from this study were in the same line with those studies using four indices (AVI, BI, SSI, and TI) to generate FCD model from Landsat TM and ETM+ images [32] [33]. The overall accuracy and Kappa coefficient were at 71-83% and 0.61-0.78 respectively. Those study corresponded to author who tested the FCD model by using three indices (AVI, BI, and SSI) from Indian remote sensing satellite (IRS) imagery 2007 of an old growth forest of the north forest division in Iran. The overall accuracy of the IRS images was at 84.4% and the Kappa coefficient reported at 0.78. [34].

The classified GVCD map in Figure 5 displays the area of medium forest class in approximately 40% of the overall forest area of Phu Phan National Park in 2015. The forest areas surrounded this National Park are the open forest class. The majority of those areas connect to agricultural fields: crop fields, rubber tree fields, and paddy fields. This area has been disturbed continuously because their boundaries connect to villages, so it is convenient to access into the National Park and easy in finding natural products and hunting wild animals. These activities cause wildfire every year. Therefore, those forest areas are considered risky to be the most degraded forests.

5. CONCLUSIONS

Spectral mixture analysis (SMA) is a sub-pixel classification technique based on the spectral responses of land cover components. SMA assumes that each image spectrum is a linear combination of a few pure spectra, so-called endmembers**.** In this study, the pixel purity index was used to select endmembers for finding the most "spectrally pure" (extreme) pixels in multispectral images. We constructed four endmembers to generate fraction images of soil, shade, green vegetation and non-photosynthetic vegetation from THAICHOTE imagery on four bands (1–4) by using spectral unmixing method. For this model, the RMSE was at 0.028.

The statistical relationship analysis between widely used vegetation indices (EVI, SAVI, NDVI, MSAVI2 and GEMI) and GV, soil fractions derived from SMA model by Pearson correlation revealed that the high correlation ($r \geq 0.96$) was also observed between GV-NDVI, GV-EVI, and GV-SAVI, except for MSAVI2 which reported as the lowest correlation between all vegetation indices. On the other hand, the relationship between soil fraction and other vegetation indices indicated that their relationship was pretty oppositely high ($r \geq 0.71$).

In this study, we demonstrated a new method based on the spatial integration which was operated by combining green vegetation fraction (GV) and soil fraction derived from SMA techniques and scaled shadow index (SSI) to create the green vegetation canopy density (GVCD) in order to classify the forest canopy density. The field survey of 48 points was used to evaluate the reliability of GVCD approach. The confusion matrix revealed that canopy classes were mapped with overall accuracy of 79.17% and with 0.68 of kappa coefficient. The dense forest class was classified more accurately with a producer's accuracy of 100% than other canopy classes.

GVCD approach is considered to be a method that could be applied to identify the green vegetation canopy density and its spatial distribution. The result of forest type classification was highly accurate. However, this method could provide the best result only in summer because the plants are in the process of shedding their leaves. Dense forest and open forest had distinct spectral signatures in remotely sensed data. GVCD approach is a quantitative measure of forest distribution provided the results with details that could be employed in the further similar studies. It is possible to apply in the detection and analysis land cover/land use changes, deforestation and forest degradation.

ISSN: 1992-8645 www.jatit.org E-ISSN: 1817-3195

6. ACKNOWLEDGEMENTS

The author would like to thank the Geo-Informatics and Space Technology Development Agency organization (GISTDA) who support THAICHOTE data. Additionally, support was provided by Faculty of Science, Khon Kaen University.

REFRENCES:

[1] P. R. Coppin and M. E. Bauer, "Processing of Multitemporal Landsat TM Imagery to Optimize Extraction of Forest Cover Change Features", *IEEE Transactions on Geoscience and Remote Sensing*, Vol. 32, No. 4, 1994, pp. 918–927.

[2] A. Rikimaru, P. S. Roy, and S. Miyatake, "Tropical forest cover density mapping", *Tropical Ecology*, Vol. 43, No. 1 June, 2002, pp. 39–47.

[3] S. Nandy, P. K. Joshi, and K. K. Das, "Forest canopy density stratification using biophysical modeling", *Journal of the Indian Society of Remote Sensing*, Vol. 31, No. 4, 2003, pp. 291–297.

[4] M. S. Mon, N. Mizoue, N. Z. Htun, T. Kajisa, and S. Yoshida, "Estimating forest canopy density of tropical mixed deciduous vegetation using Landsat data: A comparison of three classification approaches", *International Journal of Remote Sensing*, Vol. 33, No. 4, 2012, pp. 1042–1057.

[5] J. Deka, O. P. Tripathi, and M. L. Khan, "Implementation of Forest Canopy Density Model to Monitor Tropical Deforestation", *Journal of the Indian Society of Remote Sensing*, Vol. 41, No. 2, 2013, pp. 469–475.

[6] J. Kumar, P. Talwar, and K. A.P., "Forest Canopy Density and ASTER DEM based Study for Dense Forest Investigation using Remote Sensing and GIS Techniques around East Singhbhum in Jharkhand, India", *International Journal of Advanced Remote Sensing and GIS*, Vol. 4, No. 1, 2017, pp. 1026–1032.

[7] S. C. Pal, R. Chakrabortty, S. Malik, and B. Das, "Application of forest canopy density model for forest cover mapping using LISS-IV satellite data: a case study of Sali watershed, West Bengal", *Modeling Earth Systems and Environment*, Vol. 4, No. 2, 2018, pp. 853–865.

[8] J. W. Rouse, R. H. Haas, J. A. Schell, A. Deering, D.W., and J. C. Harlan, "Monitoring the vernal advancement and retrogration (Green Wave Effect) of natural vegetation.", [Online]. Available: https://ntrs.nasa.gov/search.jsp?R=19740008955 [Accessed 15 October 2018].

[9] A. R. Huete, "A soil-adjusted vegetation index (SAVI)", *Remote Sensing of Environment*, Vol. 25, No. 3, 1988, pp. 295–309.

[10] B. Pinty and M. M. Verstraete, "GEMI : A non-linear index to monitor global vegetation from satellites", *Vegetatio*, Vol. 101, No. July (1), 1992, pp. 15–20.

[11] J. Qi, A. Chehbouni, A. R. Huete, Y. H. Kerr, and S. Sorooshian, "A modified soil adjusted vegetation index", *Remote Sensing of Environment*, Vol. 48, No. 2, 1994, pp. 119–126.

[12] A. R. Huete, C. Justice, and W. van Leeuwen, "MODIS Vegetation Index (MOD13) Algorithm Theoretical Basis Document", [Online]. Available: http://modis.gsfc.nasa.gov/data/atbd/atbd_mod13.pdf [Accessed 9 November 2018].

[13] P. Fisher, "The pixel: A snare and a delusion", *International Journal of Remote Sensing*, Vol. 18, No. 3, 1997, pp. 679–685.

[14] M. O. Smith, S. L. Ustin, J. B. Adams, and A. R. Gillespie, "Vegetation in deserts. 1. A regional measure of abundance from multispectral images", *Remote Sensing of Environment*, Vol. 31, 1990, pp. 1−26.

[15] A. J. Elmore, J. F. Mustard, S. J. Manning, and D. B. Lobell, "Quantifying Vegetation Change in Semiarid Environments : Precision and Accuracy of Spectral Mixture Analysis and the Normalized Difference Vegetation Index", *Remote Sensing of Environment*, Vol. 73, No. 1, 2000, pp. 87–102.

[16] D. R. Peddle, S. P. Brunke, and F. G. Hall, "A Comparison of Spectral Mixture Analysis and Ten Vegetation Indices for Estimating Boreal Forest Biophysical Information from Airborne Data", *Canadian Journal of Remote Sensing*, Vol. 27, No. 6, 2001, pp. 627–635.

[17] D. Riaño, E. Chuvieco, S. Ustin, R. Zomer, P. Dennison, D. Roberts, and J. Salas, "Assessment of vegetation regeneration after fire through multitemporal analysis of AVIRIS images in the Santa Monica Mountains", *Remote Sensing of Environment*, Vol. 79, No. 1, 2002, pp. 60–71.

[18] D. Lu, E. Moran, and M. Batistella, "Linear mixture model applied to Amazonian vegetation classification", *Remote Sensing of*

Environment, Vol. 87, 2003, pp. 456–469.

[19] D. Lu, M. Batistella, E. Moran, and P. Mausel, "Application of spectral mixture analysis to Amazonian land-use and land-cover classification", *International Journal of Remote Sensing*, Vol. 25, No. 23, 2004, pp. 5345–5358.

[20] D. Gudex-Cross, J. Pontius, and A. Adams, "Enhanced forest cover mapping using spectral unmixing and object-based classification of multi-temporal Landsat imagery", *Remote Sensing of Environment*, Vol. 196, 2017, pp. 193–204.

[21] C. M. Souza *et al.*, "Ten-year landsat classification of deforestation and forest degradation in the brazilian amazon", *Remote Sensing*, Vol. 5, No. 11, 2013, pp. 5493–5513.

[22] A. A. M. Salih, E. T. Ganawa, and A. A. Elmahl, "Spectral mixture analysis (SMA) and change vector analysis (CVA) methods for monitoring and mapping land degradation/desertification in arid and semiarid areas (Sudan), using Landsat imagery", *The Egyptian Journal of Remote Sensing and Space Sciences*, Vol. 20, 2017, pp. S21–S29.

[23] R. C. Grecchi *et al.*, "An integrated remote sensing and GIS approach for monitoring areas affected by selective logging: A case study in northern Mato Grosso, Brazilian Amazon", *International Journal of Applied Earth Observation and Geoinformation*, Vol. 61, 2017, pp. 70–80.

[24] G. Chander, B. L. Markham, and D. L. Helder, "Summary of current radiometric calibration coefficients for Landsat MSS, TM, ETM+, and EO-1 ALI sensors", *Remote Sensing of Environment*, Vol. 113, No. 5, 2009, pp. 893–903.

[25] A. J. McDonald, F. M. Gemmell, and P. E. Lewis, "Investigation of the utility of spectral vegetation indices for determining information on coniferous forests", *Remote Sensing of Environment*, Vol. 66, No. 3, 1998, pp. 250–272.

[26] A. N. Rencz, "*Remote sensing of the earth sciences. Manual of Remote Sensing*", American Society for Photogrammetry and Remote Sensing., 1999, pp. 251–306.

[27] D. Roberts, G. Batista, J. Pereira, E. Waller, and B. Nelson, "*Change identification using multitemporal spectral mixture analysis: Applications in eastern Amazonia*", Remote Sensing Change Detection: Environmental Monitoring Applications and Methods, R.S. Lunetta and C.D. Elvidge (Eds), 1998, pp. 137–161.

[28] J. B. Adams, D. E. Sabol, V. Kapos, R. A. Filho, D. A. Roberts, M. O. Smith, and A. R. Gillespie, "Classification of Multispectral Images Based on Fractions of Endmembers : Application to Land-Cover Change in the Brazilian Amazon", *Remote Sensing of Environment*, Vol. 52, No. 2, 1995, pp. 137–154.

[29] J. W. Boardman, F. a. Kruse, and R. O. Green, "Mapping target signatures via partial unmixing of AVIRIS data," *Summaries Proceedings of the Fifth JPL Airborne Earth Science Workshop*, 1995, pp. 95-101.

[30] A. Rikimaru and S. Miyatake, "Development of Forest Canopy Density Mapping and Monitoring Model using Indices of Vegetation, Bare soil and Shadow", [Online]. Available:https://www.geospatialworld.net/article/development-of-forest-canopy-density-mapping-and-monitoring-model-using-indices-of-vegetation-bare-soil-and-shadow/ [Accessed 19 May 2018].

[31] E. A. T. Matricardi, D. L. Skole, M. A. Pedlowski, W. Chomentowski, and L. C. Fernandes, "Assessment of tropical forest degradation by selective logging and fire using Landsat imagery", *Remote Sensing of Environment*, Vol. 114, No. 5, 2010, pp. 1117–1129.

[32] M. S. Jamalabad and A. A. Abkar, "Forest canopy density monitoring, using satellite images", *Proceeding. of The International Society for Photogrammetry and Remote Sensing Congress,* 2004, pp. 12–23.

[33] E. Pakkhesal and A. E. Bonyad, "Classification and delineating natural forest canopy density using FCD Model (case study: Shafarud area of Guilan)", *Iranian Journal of Forest and Poplar Research*, Vol. 21, No. 1, 2013, pp. 99–114.

[34] Z. Azizi, A. Najafi, and H. Sohrabi, "Forest canopy density estimating using satellite images," *The International Archives of the Photogrammetry, Remote Sensing and Spatial Information Sciences Conference*, 2008.

Journal of Theoretical and Applied Information Technology
15th July 2019. Vol.97. No 13

ISSN: 1992-8645 www.jatit.org E-ISSN: 1817-3195

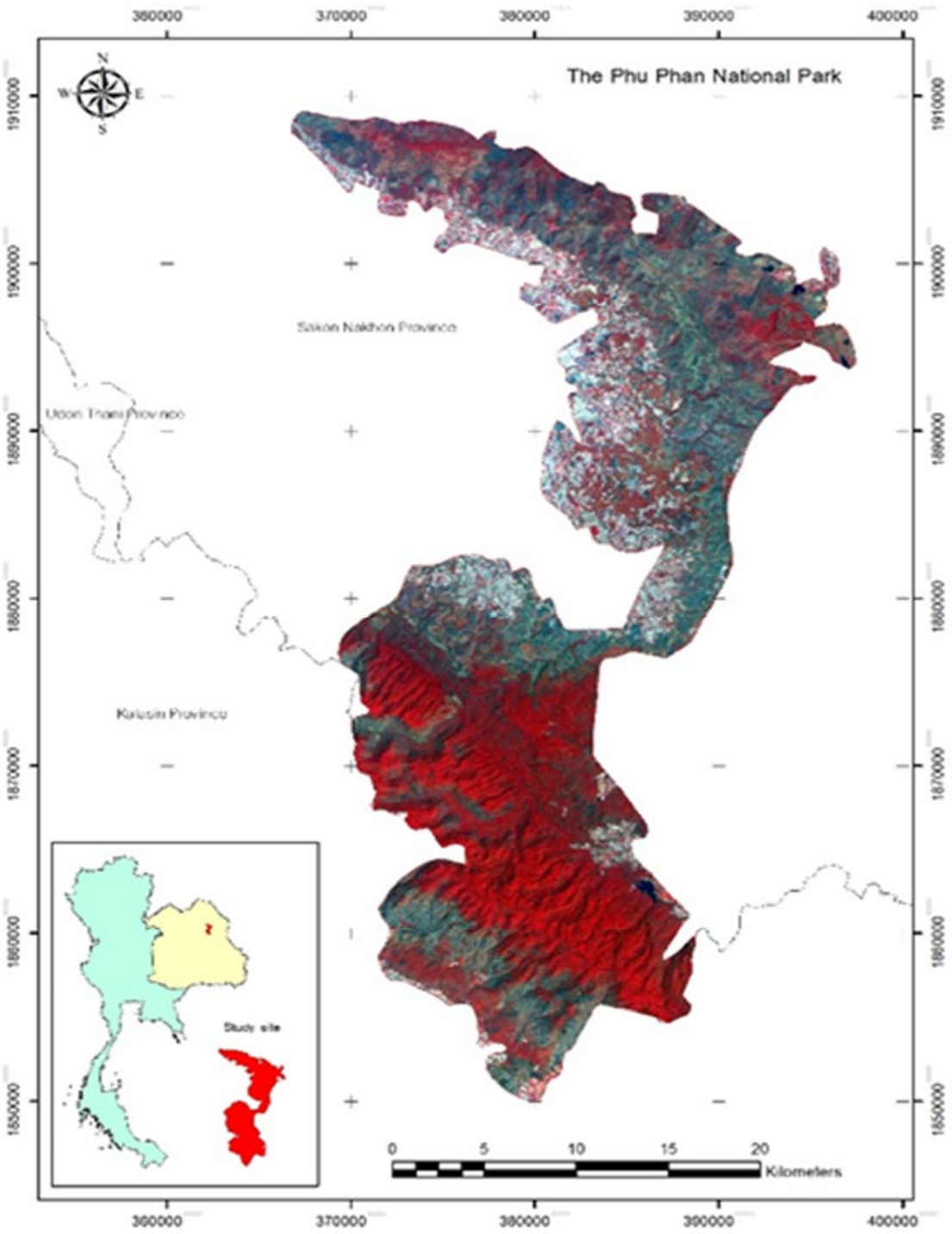

Figure 1 : Study site

ISSN: 1992-8645 www.jatit.org E-ISSN: 1817-3195

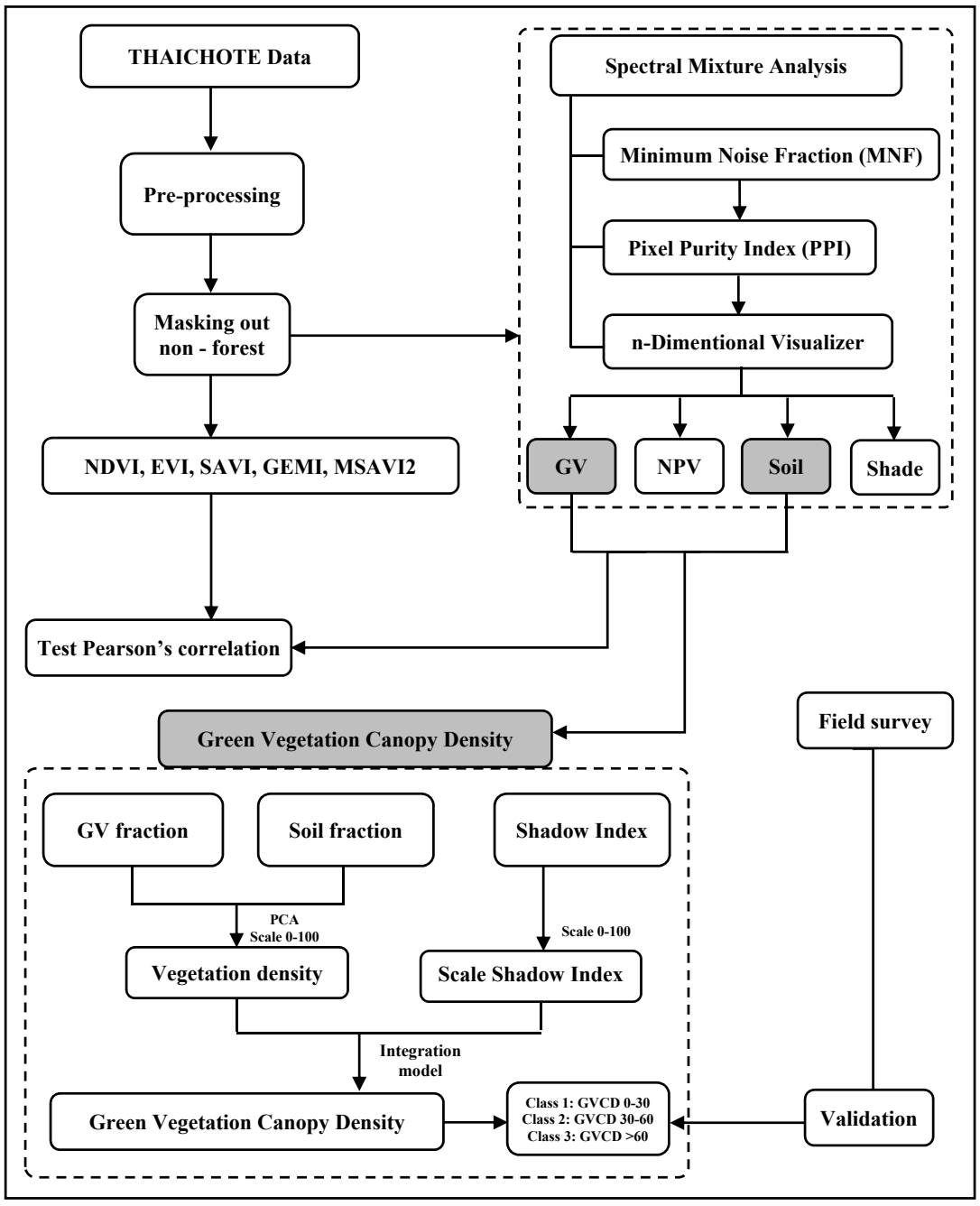

Figure 2: The flowchart of this study.

ISSN: 1992-8645 www.jatit.org E-ISSN: 1817-3195

Table 2: Correlation matrix

Vegetation index	EVI	SAVI	NDVI	MSAVI2	GEMI	GV	SOIL
EVI	1						
SAVI	0.99	1					
NDVI	0.99	0.99	1				
MSAVI2	0.06	0.06	0.03	1			
GEMI	0.98	0.99	0.97	0.11	1		
GV	0.97	0.96	0.98	-0.05	0.92	1	
SOIL	-0.71	-0.74	-0.76	-0.08	-0.71	-0.73	1

Correlation is significant at the 0.01 level (2-tailed).

Table 3: Accuracy assessment results for forest classification techniques.

Classified data	Ground truth				Producer's Accuracy	User's Accuracy
	Open Forest	Medium Forest	Dense Forest	Total		
Open Forest	16	2	0	18	76.19%	88.88%
Medium Forest	4	11	0	15	68.75%	73.33%
Dense Forest	1	3	11	15	100.0%	73.33%
Total	21	16	11	48	-	-
Error of omission	23.81%	31.25%	0.00%	-	-	-
Error of commission	7.41%	12.50%	10.81%	-	-	-

Overall classification accuracy = 79.17%.
Kappa statistics = 0.68.

ISSN: 1992-8645 www.jatit.org E-ISSN: 1817-3195

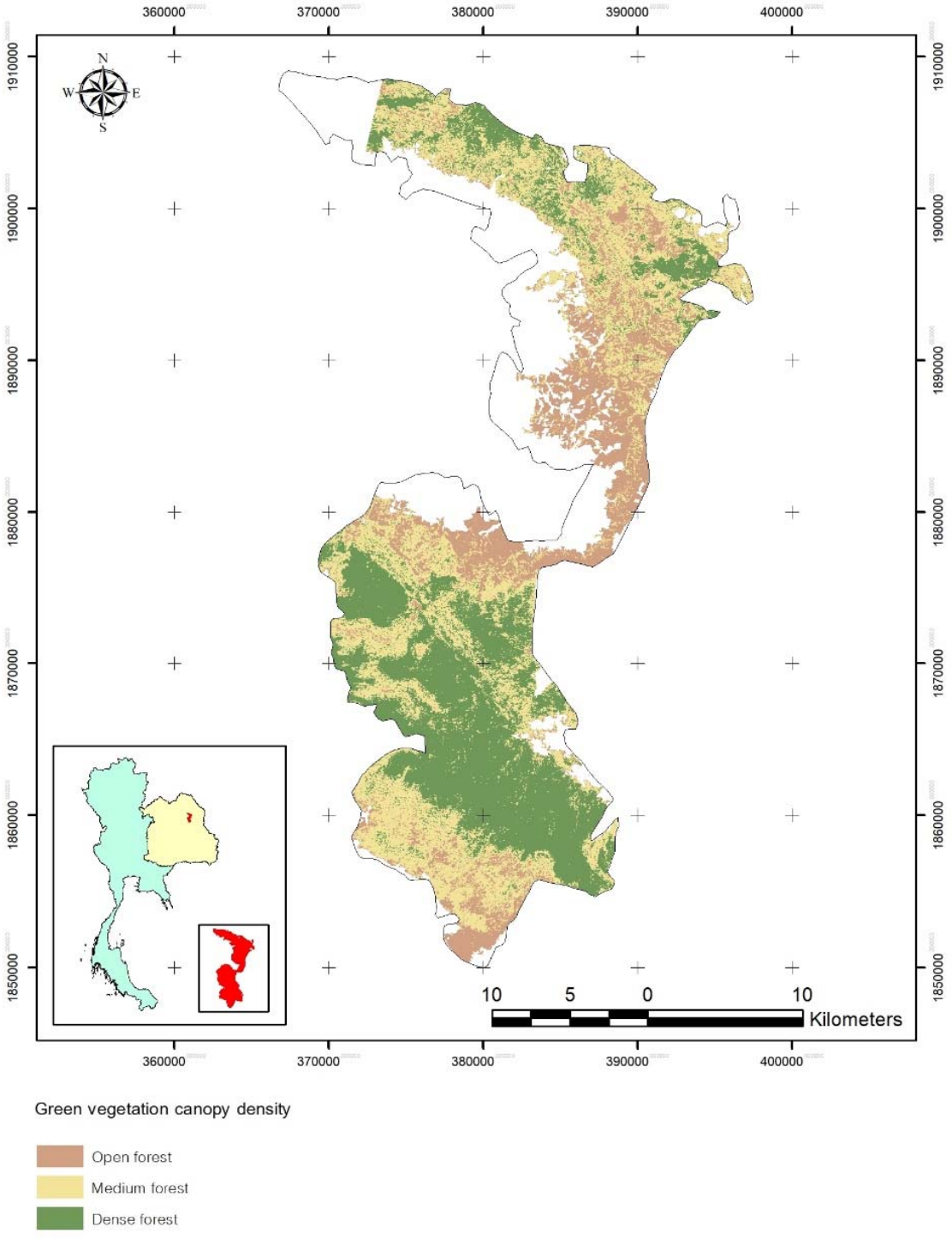

Figure 5: Green vegetation canopy density in 2015.